Bull Mater Sci (2020) 43:253
https://doi.org/10.1007/s12034-020-02228-x

Facile low-temperature synthesis of W-rich $Cu_{1-x}Zn_xWO_4$ nanoparticles and the electrochemical performance

V BALASUBRAMANIAN[1], T DANIEL[1], J HENRY[1], G SIVAKUMAR[2] and K MOHANRAJ[1,*]

[1]Department of Physics, Manonmaniam Sundaranar University, Tirunelveli 627 012, India
[2]CISL, Department of Physics, Annamalai University, Annamalai Nagar 608 002, India
*Author for correspondence (kmohanraj.msu@gmail.com; mohanraj@msuniv.ac.in)

MS received 7 December 2019; accepted 16 March 2020

Abstract. This paper reports the facile low-temperature synthesis of $Cu_{1-x}Zn_xWO_4$ nanoparticles by varying the concentration of Zn using solid-state reaction method. The incorporation of various Zn concentrations can alter the valence band energy and enhance the structural, optical and electrochemical properties. The prepared nanoparticles have a triclinic crystal structure with minimum strain. The variation in zinc concentration is shown by the densely aggregated particles in the SEM image. These nanoparticles exhibit strong absorption in the visible region and the bandgap is found to increase with an increase in Zn concentration. The photocurrent density increases with an increase in the concentration of zinc and found to be a maximum of 8.5 μA cm^{-2} for $x = 0.4$ due to a lower bandgap of 2.65 eV. Finally, it is observed that an optimum zinc concentration promotes improved photocurrent generation.

Keywords. Copper zinc tungstate; nanoparticles; aggregation; electrical properties; photocurrent.

1. Introduction

Copper tungstate ($CuWO_4$) is a promising photocatalytic material that absorbs more visible light in the solar spectrum. It is an n-type semiconductor that has an energy bandgap of 2.2 to 2.4 eV and it is widely used as an electrocatalyst for O_2 and CO_2 reduction [1], lithium-ion batteries [2], water splitting [3], gas sensors [4] and hydrogen generation [5]. Recent studies on $CuWO_4$ have shown its potential as a water oxidation photoanode but the measured photocurrent is limited due to an increased bandgap of 2.5 eV and electrode stability [6]. $CuWO_4$ nanostructures can be tailored by adding a dopant Zn^{2+} into the metal oxide which results in increased absorption of visible light. The natural advantages of Zn are high electronic conduction, low cost, non-toxicity and chemical stability. Moreover, the ionic radius of Zn^{2+} is comparable with Cu^{2+} and hence it can be exactly incorporated into the Cu lattice. Salimi *et al* [7] synthesized Ag functionalized $CuWO_4/WO_3$ nanocomposites for solar water splitting and obtained a 3–4 fold higher photocurrent density compared to pristine $CuWO_4$. Ma *et al* [8] studied the photocatalytic activity of $Cu_{1-x}Zn_xWO_4/ZnWO_4$ hybrid material and reported a bandgap of about 2.1 eV. Even though the dopant improves the optical properties of $CuWO_4$, it is necessary to analyse the effect of Zn concentration on both structural and optical properties to improve the photoconversion efficiency. To circumvent these limitations, it is essential to optimize the concentration of adding the Zn dopant in $CuWO_4$ without any defects.

In this research study, a facile solid-state reaction is adopted to synthesize copper zinc tungsten oxide ($Cu_{1-x}Zn_xWO_4$) by varying the concentration of Zn ($x = 0.2$–0.4). Though there are various chemical methods available for the preparation of these nanoparticles, the release of unwanted gases during the formation of nanoparticles may affect human health and environment. Dorfman *et al* [9] reported that CuO and WO_3 can completely transform into $CuWO_4$ with a minimum annealing temperature of 800°C. Notably, we prepare the copper zinc tungsten oxide nanoparticles by annealing it at a low temperature of about 600°C. Hence, it is essential to optimize the concentration of the zinc dopant by analysing the structural, morphological, optical and electrical properties.

2. Experimental

Copper(II) oxide (CuO), tungsten oxide (WO_3) and zinc oxide (ZnO) with 99.9% purity were used throughout the synthesis process for obtaining $Cu_{1-x}Zn_xWO_4$ by the traditional solid-state reaction method by varying the concentration of zinc. First, the metal oxide samples were well

Electronic supplementary material: The online version of this article (https://doi.org/10.1007/s12034-020-02228-x) contains supplementary material, which is available to authorized users.

Published online: 02 September 2020

ground for 1 h using mortar and pestle. Then the wellground mixture was transferred into an alumina crucible which was kept in a muffle furnace maintaining the temperature at 600°C for 3 h. Then it was allowed to cool within the furnace itself. After the annealing, we obtained green-coloured particles. The samples $x = 0.2$, 0.3 and 0.4 are named $Cu_{0.8}Zn_{0.2}WO_4$, $Cu_{0.7}Zn_{0.3}WO_4$ and $Cu_{0.6}Zn_{0.4}WO_4$, respectively. The structural analysis was carried out using (PANalytical XPERT-PRO) X-ray diffractometer and Perkin-Elmer FTIR spectrometer (Spectrum Two, Model: C92107) with the resolution of 4 cm^{-1}. The optical studies were performed using Shimadzu UV-2700. A JEOL-JSM 5610LV scanning electron microscope was used to analyse the surface morphology. Photoelectrochemical (PEC) measurements were performed in a PEC cell using CH 604E electrochemical workstation.

3. Results and discussion

The reaction mechanism involved in the solid-state reaction can be understood by the following equation:

$$(1-x)\mathrm{CuO} + x\mathrm{ZnO} + \mathrm{WO_3} \longrightarrow \mathrm{Cu_{1-x}Zn_xWO_4} \qquad (1)$$

The XRD pattern of $Cu_{1-x}Zn_xWO_4$ nanoparticles is shown in figure 1. At $x = 0.2$, the high-intensity peak observed at $2\theta = 30.22°$ belongs to (1–11) plane whereas earlier reports for pristine $CuWO_4$ shows the major peak at $2\theta = 28.78°$ [10]. The shift in the angle confirms the incorporation of Zn into $CuWO_4$. All the peaks obtained were well matched with the standard JCPDS (88-0265) of $Cu_{0.8}Zn_{0.2}WO_4$. At $x = 0.3$ and $x = 0.4$, the major peak is shown at $2\theta = 30.22°$ and $2\theta = 30.84°$ and belong to (020) plane. Two additional peaks have also appeared for $x = 2$ at $2\theta = 32.20°$ and $2\theta = 33.37°$ with lower intensity and the remaining peaks matched with the JCPDS (88-0263) of $Cu_{0.7}Zn_{0.3}WO_4$ whereas $x = 4$ matches with the JCPDS card (88-0261). However, at $x = 0.4$, additional peaks were found at $2\theta = 24.40°$ and $2\theta = 33.29°$. These additional peaks are attributed to the formation of WO_3 which also confirms the W-rich nature.

All the samples exhibit improved crystallinity having the same triclinic crystal structure. Moreover, the sharp peaks present on the entire pattern may indicate the lower microstrain and defect-free crystal system [11]. Besides, no change in phase was observed but the intensity of the major peaks increased on increasing the concentration of Zn^{2+}. The calculated crystallite size, dislocation density and microstrain of $Cu_{1-x}Zn_xWO_4$ is given in table 1.

Figure 2 shows the SEM images of $Cu_{1-x}Zn_xWO_4$ nanoparticles annealed at 600°C. On closer inspection of $Cu_{0.8}Zn_{0.2}WO_4$ (figure 2a), the formation of needles on the surface of the highly aggregated particles is evident. These observations strongly suggested the incorporation of Zn into $CuWO_4$ while in the higher magnification image (figure 2b), the presence of aggregate is accompanied by small gaps between the needles that confirm the mesoporous structure. On increasing the Zn concentration ($x = 0.3$) of $Cu_{0.7}Zn_{0.3}WO_4$, the aggregation becomes highly dense. It is due to the inclusion of Zn^{2+} ions that diffuse into lattice sites of Cu^{2+} that have a similar ionic radius and hence, the particles are assembled in the form of blocks. A further increase in the concentration at $x = 0.4$, clearly depicted the incorporation of more number of Zn^{2+} ions. Apart from these observations, the mesoporous structure disappeared on increasing the Zn^{2+} concentration [12]. It is an important strategy that these particles have potential applications in the field of electrochemistry. The EDX analysis was also performed to confirm the existence of Cu, W, O and Zn elements as given in supporting information. The EDX spectrum shows W-rich nature of $Cu_{1-x}Zn_xWO_4$ nanoparticles as shown in figures S1–S3.

The UV–Vis absorption spectra of $Cu_{1-x}Zn_xWO_4$ nanoparticles are shown in figure 3. From the absorption spectra shown, the variation in zinc concentration is evidenced by the shifted peaks from 450 nm towards the longer

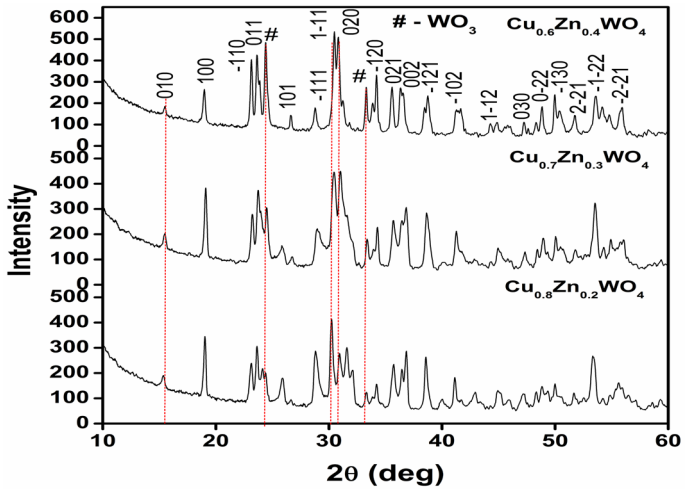

Figure 1. XRD pattern of $Cu_{1-x}Zn_xWO_4$ nanoparticles.

Table 1. Crystallite size, microstrain and dislocation density of $Cu_{1-x}Zn_xWO_4$ nanoparticles.

Sample	Crystallite size (nm)	Microstrain	Dislocation density (lines m^{-2})
$Cu_{0.8}Zn_{0.2}WO_4$	63	0.011	2.51×10^{14}
$Cu_{0.7}Zn_{0.3}WO_4$	41	0.015	5.94×10^{14}
$Cu_{0.6}Zn_{0.4}WO_4$	47	0.012	4.52×10^{14}

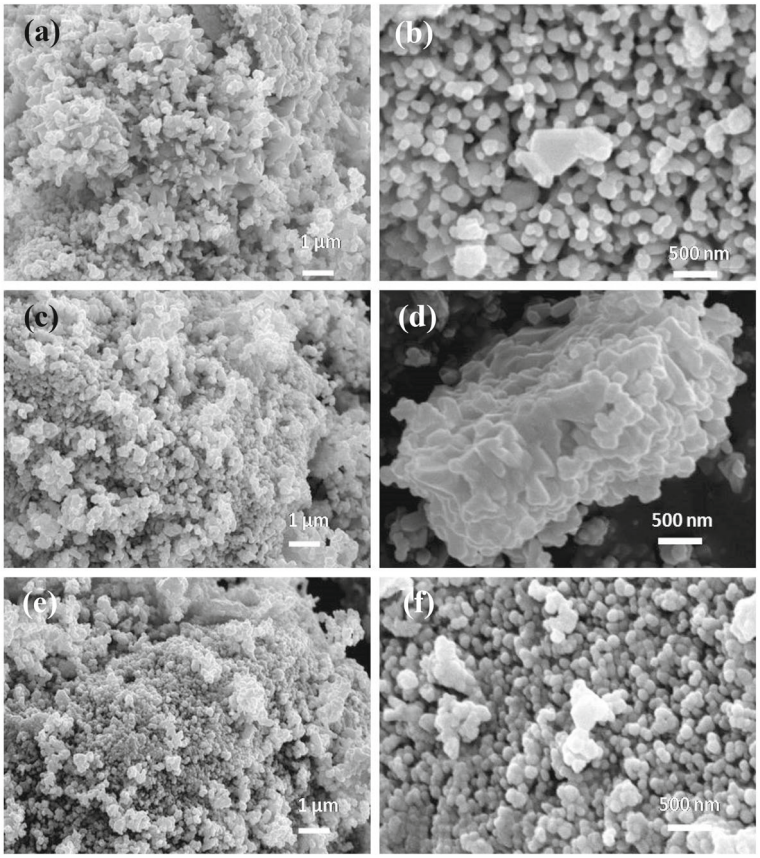

Figure 2. SEM images of $Cu_{1-x}Zn_xWO_4$ nanoparticles: (**a** and **b**) $x = 0.2$, (**c** and **d**) $x = 0.3$, (**e** and **f**) $x = 0.4$.

wavelength. All the nanoparticles exhibited maximum absorption in the visible range. There is no significant change in the absorption edges for the nanoparticles which is reflected by the nearly same morphology with strong aggregation. The aggregated particle reduces the surface-active sites and limits the bandgap.

The bandgap of the nanoparticles was calculated using the Tauc plot and it was found to be 2.69, 2.75 and 2.65 eV for $Cu_{0.8}Zn_{0.2}WO_4$, $Cu_{0.7}Zn_{0.3}WO_4$ and $Cu_{0.6}Zn_{0.4}WO_4$, respectively. The enlarged bandgap compared to bare $CuWO_4$ is significantly due to the Zn ions which possess elevated conduction band levels. The bandgap is an important tool that affects the PEC efficiency of the material. Despite the higher bandgap, these particles have great potential applications in the field of photoelectrochemistry due to the maximum absorption of visible light in the solar spectrum.

The PEC measurements were performed in a three electrode cell using 0.1 M of Na_2SO_4 which acts as a suitable electrolyte with the illumination intensity of 100 mW cm^{-2}. The J–V plots drawn for $Cu_{0.8}Zn_{0.2}WO_4$, $Cu_{0.7}Zn_{0.3}WO_4$ and $Cu_{0.6}Zn_{0.4}WO_4$ electrode are shown in figure 4. It shows a significant photocurrent increase in the overall potential range and with a maximum of about 8.5 µA cm^{-2} for $x = 0.4$. In the case of $x = 0.2$ and $x = 0.3$, it is found to be lower at about 6.6 and 4.9 µA cm^{-2}. Moreover, lower oxidation current is observed in the potential range up to 0.1 V in the dark indicating that the electrode is not active for oxygen evolution reaction.

But under illumination, a large oxidation photocurrent is observed due to PEC oxygen evolution reaction [13]. It is observed from this result that the photocurrent increases with an increase in the concentration of zinc. However, for

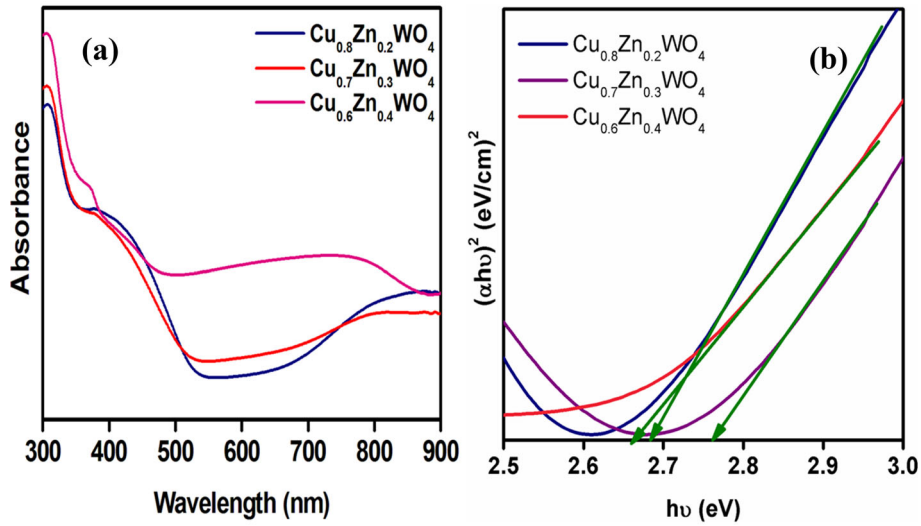

Figure 3. (**a**) UV–Vis spectra and (**b**) Tauc plot of $Cu_{1-x}Zn_xWO_4$ nanoparticles.

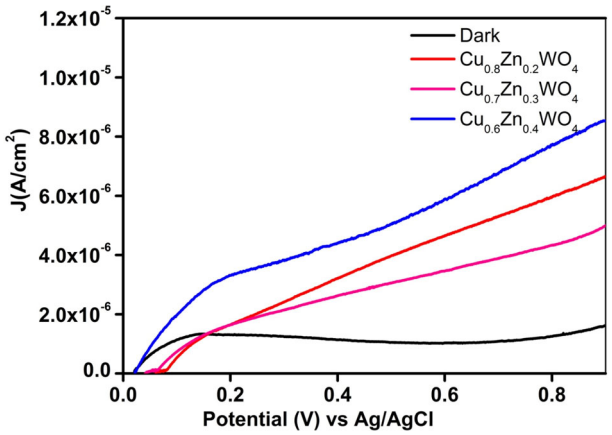

Figure 4. J–V curve of $Cu_{1-x}Zn_xWO_4$ nanoparticles.

$x = 0.3$ the current decreases when compared to $x = 0.2$ due to an increase in the bandgap of 2.63 eV. Nevertheless, the effect of Zn^{2+} in the surface of $CuWO_4$ has increased the efficiency of photoelectrode. Hence, it is clear that the sample with a higher concentration of Zn ($Cu_{0.6}Zn_{0.4}WO_4$) acts as a suitable material for increased PEC current generation. Further increase in photocurrent is achieved by optimizing the electrode preparation condition with high conductivity.

4. Conclusion

In this research study, $Cu_{1-x}Zn_xWO_4$ nanoparticles were synthesized by varying the concentration of Zn using solid-state reaction method. The XRD pattern confirms the triclinic crystal structure obtained with significant variation in crystallite size. The major crystalline peaks were shifted to a higher angle on increasing the concentration of zinc. SEM images displayed the highly aggregated particles which confirm the variation of Zn in the $CuWO_4$ lattice. These particles have potential impact in PEC properties due to increased mesoporous structure. The bandgap of the material is calculated in the range of 2.6–2.7 eV for all nanoparticles without much variation. The obtained photocurrent at a maximum of 8.5 μA cm^{-2} for higher zinc concentration ($x = 0.4$) under 1 sun illumination evidenced that these $Cu_{1-x}Zn_xWO_4$ nanoparticles have great potential for applications in photoelectrochemistry. Hence it is concluded that $Cu_{0.6}Zn_{0.4}WO_4$ is found to be optimum for increased photocurrent generation. However, further investigation is needed to improve the photocurrent generation and the efficiency of PEC cell by varying the zinc concentration $x \geq 0.4$ in $Cu_{1-x}Zn_xWO_4$ for comparing the results with commercialized PEC cells.

Acknowledgement

V Balasubramanian acknowledges DST-SERB, New Delhi, for providing financial support under Extra Mural Research (F. No. EMR/2017/000351) fund.

References

[1] Nam K M, Cheon E A, Shin W J and Bard A J 2015 *Langmuir* **39** 10897
[2] Li C L and Fu Z W 2008 *Electrochim. Acta* **12** 4293
[3] Yourey J E and Bartlett B M 2011 *J. Mater. Chem.* **21** 7651
[4] Gonzalez C M, Du X, Dunford J L and Post M L 2012 *Sens. Actuators B Chem.* **173** 169
[5] Gaillard N, Chang Y, Braun A and DeAngelis A 2012 *Mater. Res. Soc. Symp. Proc.* **1446** 19

[6] Yourey J E, Pyper K J, Kurtz J B and Bartlett B M 2013 *J. Phys. Chem. C* **17** 8708
[7] Salimi R, Alvani A S, Mei B T, Naseri N, Du S F and Mul G 2019 *New J. Chem.* **5** 2196
[8] Ma L, Su J, Liu M, Zhang L, Li Y and Guo L 2016 *J. Mater. Res.* **11** 1616
[9] Dorfman L, Houck D, Scheithauer M, Dann J and Fassett H J 2001 *Mater. Res.* **16** 1096
[10] Hill J C and Choi K S 2013 *J. Mater. Chem. A* **16** 5006
[11] Sam S R, Rayar S L and Selvarajan P 2015 *J. Chem. Pharm. Res.* **7** 957
[12] Tang Y, Rong N, Liu F, Chu M, Dong H, Zhang Y *et al* 2016 *Appl. Surf. Sci.* **361** 133
[13] Hu D, Diao P, Xu D, Xia M, Gu Y, Wu Q *et al* 2016 *Nanoscale* **11** 5892